Coport: A New Public Code for Polarized Radiative Transfer in a Covariant Framework

郭敏勇

北京师范大学

@ 2024 引力与宇宙学专题研讨会
彭桓武高能基础理论研究中心

Based on arXiv: 2407.10431, published in JCAP
Collaborate with: 黄杰伟, 郑力恒, 陈斌

November, 17, 2024

北京師範大學 物理与天文学院
SCHOOL OF PHYSICS AND ASTRONOMY, BEIJING NORMAL UNIVERSITY

Contents

Introduction

Introduction

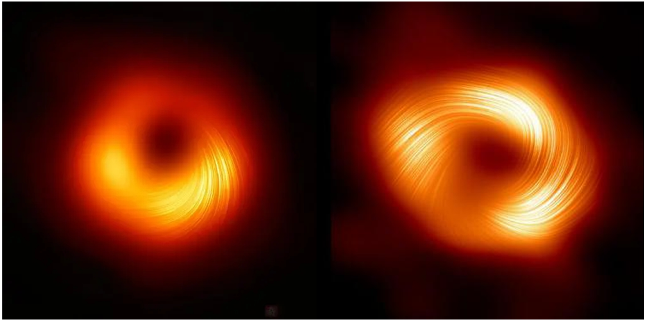

图 1: The captured images of black holes using the Event Horizon Telescope (EHT) not only reveals the intensity distribution but also provides crucial details about the polarization of light rays.

Introduction

- To understand the polarized images of black holes theoretically, it is essential to use general relativistic radiative transfer (GRRT) techniques for imaging their accreting plasma. This makes GRRT an indispensable cornerstone technology in the study of black hole images.

Introduction

- To understand the polarized images of black holes theoretically, it is essential to use general relativistic radiative transfer (GRRT) techniques for imaging their accreting plasma. This makes GRRT an indispensable cornerstone technology in the study of black hole images.
- When calculating the total intensity of a light source, the process within GRRT is relatively straightforward. It involves solving the geodesic equations for light rays and an additional radiative transfer equation to determine the intensity.

$$k^\mu \nabla_\mu k^\nu = 0 \tag{1}$$

$$\frac{d}{d\lambda}\left(\frac{I_\nu}{\nu^3}\right) = \frac{j_\nu - \alpha_\nu I_\nu}{\nu^2} \tag{2}$$

where k^μ is the wave vector for photons, λ is the affine parameter along the null geodes, I_ν is the specific intensity, α_ν is the absorption coefficient of the plasma, and j_ν is the emissivity of radiation.

Introduction

- However, the complexity in crafting the polarization images of a black hole increases to another level.

Introduction

- However, the complexity in crafting the polarization images of a black hole increases to another level.
- We need to consider both the polarization computations for both spacetime propagation and plasma propagation.

Introduction

- For the spacetime propagation, one has

$$k^\mu \nabla_\nu f^\nu = 0 \tag{3}$$

where f^μ is the polarization vector, that is, f^μ parallel-transported along the null geodesic.

Introduction

- For the spacetime propagation, one has

$$k^\mu \nabla_\nu f^\nu = 0 \tag{3}$$

where f^μ is the polarization vector, that is, f^μ parallel-transported along the null geodesic.

- In the local frame, the local Stokes parameters follow the evolution equation given below

$$\frac{\mathrm{d}}{\mathrm{d}\lambda}\begin{pmatrix}\mathcal{I}\\ \mathcal{Q}\\ \mathcal{U}\\ \mathcal{V}\end{pmatrix} = \frac{1}{\omega^2}\begin{pmatrix}j_I\\ j_Q\\ j_U\\ j_V\end{pmatrix} - \omega\begin{pmatrix}a_I & a_Q & a_U & a_V\\ a_Q & a_I & r_V & -r_U\\ a_U & -r_V & a_I & r_Q\\ a_V & r_U & -r_Q & a_I\end{pmatrix}\begin{pmatrix}\mathcal{I}\\ \mathcal{Q}\\ \mathcal{U}\\ \mathcal{V}\end{pmatrix}, \tag{4}$$

where, $\omega = -k_\mu u^\mu$ represents the frequency of photons as observed by a co-moving observer within the fluid.

Introduction

- In the field of ray-tracing code for covariant, polarized radiative transport, there are several frameworks currently in use, including grtrans, ipole, RAPTOR, Odyssey, and BHOSS.

Introduction

- In the field of ray-tracing code for covariant, polarized radiative transport, there are several frameworks currently in use, including grtrans, ipole, RAPTOR, Odyssey, and BHOSS.

- A common feature among these computational methods is the separation of equations governing the gravitational influence on light rays from those describing the interaction of light rays with the plasma. Initially, the parallel transport of the polarization vector along null geodesics in curved spacetime are solved, disregarding plasma effects. The updated polarization vector is then used as input for the next stage. This process continues by applying the evolution equations for the Stokes parameters in flat spacetime within the fluid regime, ultimately leading to the final outcomes. Nevertheless, there are distinctions in the specific handling of details.

Introduction

- A distinctive approach is seen in ipole, which originates from a covariant equation that couples both gravitational and plasma influences [Charles F. Gammie and Po Kin Leung 2012 ApJ 752 123]. However, in its implementation, ipole separates the coupled equations into gravitational and plasma components, thus adopting a two-step process within sufficiently small steps.

Introduction

- A distinctive approach is seen in ipole, which originates from a covariant equation that couples both gravitational and plasma influences [Charles F. Gammie and Po Kin Leung 2012 ApJ 752 123]. However, in its implementation, ipole separates the coupled equations into gravitational and plasma components, thus adopting a two-step process within sufficiently small steps.

- In light of the covariant equation that intertwines gravitational and plasma influences, we aim to give a novel approach and develop **Coport** that achieves a unified evolution of the coupled equations. Different from ipole, we do not try to decouple the covariant equation into two components.

The framework of **Coport**

The framework of **Coport**

- To describe the interaction between light rays and matter in radiative transfer, this study employs the tensor form of the radiative transfer equation as presented in [Charles F. Gammie and Po Kin Leung 2012 ApJ 752 123]

$$k^\mu \nabla_\mu \mathcal{S}^{\alpha\beta} = \mathcal{J}^{\alpha\beta} + H^{\alpha\beta\mu\nu}\mathcal{S}_{\mu\nu} \,. \tag{5}$$

Here, k^μ is the wave vector for photons, $\mathcal{J}^{\alpha\beta}$ characterizes the emission from the source, and $H^{\alpha\beta\mu\nu}$ represents absorption and Faraday rotation effects. The quantity $\mathcal{S}^{\alpha\beta}$, referred to as the polarization tensor, describes polarization as a Hermitian tensor, satisfying $\mathcal{S}^{\alpha\beta} = \bar{\mathcal{S}}^{\beta\alpha}$, where the bar denotes complex conjugation. The details on the derivation of Eq. (5), as well as the definitions of $H^{\alpha\beta\mu\nu}$ and the properties of $\mathcal{S}^{\alpha\beta}$, can be found in Appendix A of our paper.

The framework of **Coport**

- In practical computations, particularly when analyzing accretion disk material near black holes, it is crucial to establish a specific frame of reference to accurately depict the emission, the absorption, and the rotation of local polarized light.

The framework of **Coport**

- In practical computations, particularly when analyzing accretion disk material near black holes, it is crucial to establish a specific frame of reference to accurately depict the emission, the absorption, and the rotation of local polarized light.

- A suitable fluid coordinate system, as given in [Avery Broderick and Roger Blandford 2004 MNRAS], is adopted in this work.

The framework of **Coport**

Given a fluid four-velocity u^μ, a light ray wavenumber k^μ, and any spacelike vector d^μ, the four basis vectors of this coordinate system are respectively

$$\begin{aligned} e^\mu_{(0)} &= u^\mu \,, \quad e^\mu_{(3)} = \frac{k^\mu}{\omega} - u^\mu \,, \quad e^\mu_{(2)} = \frac{1}{\mathcal{N}}\Big(d^\mu + \beta u^\mu - C e^\mu_{(3)}\Big) \,, \\ e^\mu_{(1)} &= \frac{\epsilon^{\mu\nu\sigma\rho} u_\nu k_\sigma d_\rho}{\omega \mathcal{N}} \,, \end{aligned} \tag{6}$$

where, $\epsilon^{\mu\nu\sigma\rho}$ is the Levi-Civita tensor, with

$$\begin{aligned} d^2 &= d_\mu d^\mu \,, \quad \beta = u_\mu d^\mu \,, \quad \omega = -k_\mu u^\mu \,, \quad C = \frac{k_\mu d^\mu}{\omega} - \beta \,, \\ \mathcal{N} &= \sqrt{d^2 + \beta^2 - C^2} \,. \end{aligned} \tag{7}$$

We typically set d^μ as the local magnetic field b^μ. This choice leads to the vanishing of all emission, absorption, and rotation coefficients associated with the Stokes parameter U in the context of polarization.

The framework of **Coport**

Considering the gauge symmetry inherent in the polarization tensor $\mathcal{S}^{\alpha\beta}$, we can restrict our discussion of the tensors to the orthogonal subspace $\{e^{\mu}_{(1)}, e^{\mu}_{(2)}\}$. The projection of $\mathcal{S}^{\alpha\beta}$ within the orthogonal subspace $\{e^{\mu}_{(1)}, e^{\mu}_{(2)}\}$ is given by

$$\hat{S}^{(a)(b)} = \begin{pmatrix} \mathcal{I} + \mathcal{Q} & \mathcal{U} + i\mathcal{V} \\ \mathcal{U} - i\mathcal{V} & \mathcal{I} - \mathcal{Q} \end{pmatrix}. \tag{8}$$

Here, $\{\mathcal{I}, \mathcal{Q}, \mathcal{U}, \mathcal{V}\} = \left\{I/\nu^3, Q/\nu^3, U/\nu^3, V/\nu^3\right\}$ represent the invariant Stokes parameters. The hat notation indicates the projection in the orthogonal subspace $\{e^{\mu}_{(1)}, e^{\mu}_{(2)}\}$.

The framework of **Coport**

By comparing the projection of Eq. (5) in the rest frame of the fluid with Eq. (4), we can derive the projection of the emission tensor $\mathcal{J}^{(a)(b)}$ in the orthogonal subspace of the fluid frame, denoted by $\{e^{\mu}_{(1)}, e^{\mu}_{(2)}\}$, as follows:

$$\hat{\mathcal{J}}^{(a)(b)} = \frac{1}{\omega^2}\begin{pmatrix} j_I + j_Q & j_U + i j_V \\ j_U - i j_V & j_I - j_Q \end{pmatrix} . \tag{9}$$

Furthermore, considering

$$H^{\mu\nu\rho\sigma} = \mathcal{R}^{\mu\nu\rho\sigma} + \mathcal{A}^{\mu\nu\rho\sigma} , \tag{10}$$

the term $H^{\alpha\beta\mu\nu}$ can be decomposed into two components: one representing the absorption, denoted as $\mathcal{A}^{\alpha\beta\mu\nu}$, and the other representing the Faraday rotation, denoted as $\mathcal{R}^{\alpha\beta\mu\nu}$.

The framework of **Coport**

Next, we proceed to solve Eq. (5). First, we reformulate Equation (5) into a first-order differential equation

$$\dot{\mathcal{S}}^{\alpha\beta} = -\Gamma^{\alpha}{}_{\mu\nu} k^{\mu} \mathcal{S}^{\nu\beta} - \Gamma^{\beta}{}_{\mu\nu} k^{\mu} \mathcal{S}^{\alpha\nu} + \mathcal{J}^{\alpha\beta} + H^{\alpha\beta\mu\nu} \mathcal{S}_{\mu\nu} \,, \tag{11}$$

where, the dot denotes the differentiation with respect to the photon's affine parameter, $\frac{\mathrm{d}}{\mathrm{d}\lambda}$, while $\Gamma^{\alpha}{}_{\mu\nu}$ represents the Christoffel symbols in the corresponding coordinate system. By definition, $\mathcal{S}^{\alpha\beta}$, $\mathcal{J}^{\alpha\beta}$, and $H^{\alpha\beta\mu\nu}$ are all complex tensors. To facilitate numerical computations, our approach involves first transforming Equation (11) into a real-valued form.

The framework of **Coport**

Considering the fact that $\mathcal{S}^{\alpha\beta} = \bar{\mathcal{S}}^{\beta\alpha}$ is Hermitian, the tensor $\mathcal{S}^{\alpha\beta}$ possesses only 16 degrees of freedom. It can be decomposed into two components as follows:

$$\mathcal{S}^{\alpha\beta} = \mathcal{D}^{\alpha\beta} + i\mathcal{X}^{\alpha\beta}\,, \tag{12}$$

Here, $\mathcal{D}^{\alpha\beta} = \mathcal{D}^{\beta\alpha}$ describes the total intensity and linearly polarized light, with 10 degrees of freedom. On the other hand, $\mathcal{X}^{\alpha\beta} = -\mathcal{X}^{\beta\alpha}$ characterizes circularly polarized light, containing 6 degrees of freedom.

The framework of **Coport**

By taking the real and imaginary parts of Eq. (11), we can split it into two sets of equations:

$$\begin{aligned}
\dot{\mathcal{D}}^{\alpha\beta} &= -\Gamma^{\alpha}{}_{\mu\nu}k^{\mu}\mathcal{D}^{\nu\beta} - \Gamma^{\beta}{}_{\mu\nu}k^{\mu}\mathcal{D}^{\alpha\nu} + \mathcal{E}^{\alpha\beta} \\
&\quad + \frac{1}{2}\left(\mathcal{P}^{\alpha\mu}\mathcal{D}_{\mu}{}^{\beta} + \mathcal{D}^{\alpha\mu}\mathcal{P}^{\beta}{}_{\mu} - \mathcal{Q}^{\alpha\mu}\mathcal{X}_{\mu}{}^{\beta} + \mathcal{X}^{\alpha\mu}\mathcal{Q}^{\beta}{}_{\mu}\right), \qquad (13) \\
\dot{\mathcal{X}}^{\alpha\beta} &= -\Gamma^{\alpha}{}_{\mu\nu}k^{\mu}\mathcal{X}^{\nu\beta} - \Gamma^{\beta}{}_{\mu\nu}k^{\mu}\mathcal{X}^{\alpha\nu} + \mathcal{Y}^{\alpha\beta} \\
&\quad + \frac{1}{2}\left(\mathcal{P}^{\alpha\mu}\mathcal{X}_{\mu}{}^{\beta} + \mathcal{X}^{\alpha\mu}\mathcal{P}^{\beta}{}_{\mu} + \mathcal{Q}^{\alpha\mu}\mathcal{D}_{\mu}{}^{\beta} - \mathcal{D}^{\alpha\mu}\mathcal{Q}^{\beta}{}_{\mu}\right). \qquad (14)
\end{aligned}$$

Here, for notational convenience, we have introduced four real tensors $\mathcal{E}^{\alpha\beta}$, $\mathcal{Y}^{\alpha\beta}$, $\mathcal{P}^{\alpha\beta}$, and $\mathcal{Q}^{\alpha\beta}$, which satisfy the following conditions

$$\mathcal{E}^{\alpha\beta} = \frac{1}{2}\left(\mathcal{J}^{\alpha\beta} + \bar{\mathcal{J}}^{\alpha\beta}\right), \quad \mathcal{Y}^{\alpha\beta} = \frac{1}{2i}\left(\mathcal{J}^{\alpha\beta} - \bar{\mathcal{J}}^{\alpha\beta}\right), \qquad (15)$$

and

$$\mathcal{P}^{\alpha\beta} = \frac{1}{2}\left(\mathcal{A}^{\alpha\beta} + \bar{\mathcal{A}}^{\alpha\beta} + \mathcal{R}^{\alpha\beta} + \bar{\mathcal{R}}^{\alpha\beta}\right), \quad \mathcal{Q}^{\alpha\beta} = \frac{1}{2i}\left(\mathcal{A}^{\alpha\beta} - \bar{\mathcal{A}}^{\alpha\beta} + \mathcal{R}^{\alpha\beta} - \bar{\mathcal{R}}^{\alpha\beta}\right). \qquad (16)$$

The framework of **Coport**

Now, all quantities in Eqs. (13) and (14) have now been explicitly and concretely expressed. Consequently, we are now prepared to proceed with the resolution. Solving Eqs. (13) and (14) requires the use of a coordinate system. For non-local equations evolving in spacetime, the BL coordinate system is particularly suitable.

However, since the emission coefficient $\mathcal{J}^{\alpha\beta}$, the absorption coefficient $\mathcal{A}^{\alpha\beta}$, and the rotation coefficients $\mathcal{R}^{\alpha\beta}$ are initially provided in a local fluid system, it is essential to transform these coefficients into the ones in the BL coordinate system first. The specific procedure for this transformation is as follows. Eq. (6) allows us to express the transformation relations between the basis vectors of the fluid system and those of the BL coordinate system as follows

$$e^{\mu}_{(a)} = \Lambda^{(b)}{}_{(a)} \partial^{\mu}_{(b)} \,. \tag{17}$$

The framework of **Coport**

Subsequently, for any (2,0) type tensor $\mathcal{T}^{\mu\nu}$ mentioned earlier, the corresponding coordinate transformation is given by

$$\mathcal{T}^{\mu\nu} = \Lambda^{\mu}{}_{\rho}\tilde{\mathcal{T}}^{\rho\sigma}\Lambda^{\nu}{}_{\sigma}\,, \tag{18}$$

where, $\tilde{\mathcal{T}}^{\mu\nu}$ denotes the components of the tensor $\mathcal{T}^{ab}$ in the local fluid system, while $\mathcal{T}^{\mu\nu}$ represents its components in the BL coordinates. It is noteworthy that we can validate the results by examining the transformation of $g^{\mu\nu}$:

$$g^{\mu\nu} = \Lambda^{\mu}{}_{\rho}\tilde{\eta}^{\rho\sigma}\Lambda^{\nu}{}_{\sigma}\,. \tag{19}$$

The framework of **Coport**

After solving the equation, it is crucial to link the obtained result, $\mathcal{S}^{\alpha\beta}$, with the Stokes parameters read by the observer. To achieve this, we must establish a local frame of reference at the observer's location.

We choose a zero angular momentum observer (ZAMO) and adopt the 'looking outward' gauge to facilitate the study of polarization as shown in Fig. 2. Consequently, the frame is established as follows:

$$e_T = \frac{g_{\phi\phi}\partial_t - g_{t\phi}\partial_\phi}{\sqrt{g_{\phi\phi}\left(g_{t\phi}^2 - g_{\phi\phi}g_{tt}\right)}}\,, \quad e_X = \frac{\partial_\phi}{\sqrt{g_{\phi\phi}}}\,, \quad e_Y = -\frac{\partial_\theta}{\sqrt{g_{\theta\theta}}}\,, \quad e_Z = \frac{\partial_r}{\sqrt{g_{rr}}}\,. \tag{20}$$

The framework of **Coport**

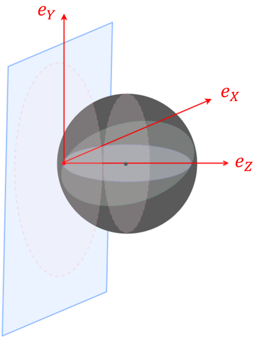

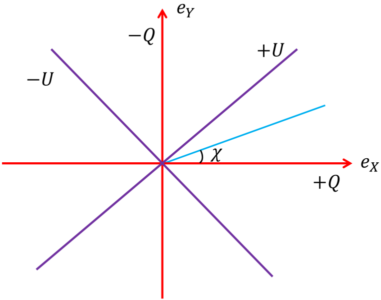

图 2: Illustration of the screen and Stokes parameters. Here, we adhere to the 'looking outward' gauge as per the IAU standards, where $e_Z \propto \partial_r$ points outward, while e_X and e_Y form the basis of the screen.

The framework of **Coport**

In our camera model, for an observer situated far from the black hole, the field of view angle is typically quite small. Consequently, we can project the polarization tensor of each pixel onto a common set of axes to derive the corresponding Stokes parameters.

By employing this projection coordinate system, we can map the values of the Stokes parameters onto the screen. These Stokes parameters are defined in accordance with IAU standards. At this stage, on the imaging plane (e_X, e_Y), the EVPA angle is given by

$$\chi = \frac{1}{2}\arctan\left(\frac{U}{Q}\right), \tag{21}$$

and the linear polarization vector can be expressed by the following equation:

$$\vec{P} = \frac{\sqrt{Q^2+U^2}}{I}(\cos\chi, \sin\chi). \tag{22}$$

The framework of **Coport**

At this point, let us summarize the entire procedure for obtaining the polarized image and Stokes Parameters using **Coport**:

1. **Backward Ray-Tracing:** Initially, we employ the backward ray-tracing technique to trace null geodesics from the observer's standpoint backward in time. This allows us to determine the endpoints of the light rays and identify whether they are captured by the black hole or continue towards infinity.
2. **Forward Progression and Radiation Transfer:** Starting from the endpoints identified in the previous step, we then trace the light rays forward in time while simultaneously solving the radiation transfer equations (13) and (14).
3. **Projection and Stokes Parameters:** We continue this process until the light rays return to the observer. At this point, we project the polarization tensor onto the observer's screen, thereby derive the Stokes parameters as read by the observer.

Numerical scheme and code verification

Numerical scheme and code verification

Our validation process is divided into four segments: the validation against analytical solutions, the thin-disk validation, the analytical thick-disk validation, and the validation of thick-disk models generated by GRMHD simulations.

In our computations, we use a Kerr black hole with a spin parameter $a = 0.94$. It is important to note that our code can be applied to any spacetime.

For the observing frequency, we choose $\nu_o = 230\,\mathrm{GHz}$, which corresponds to the actual observation frequency of the EHT.

Validation of analytical results

Our first test problem involves validating the results of the constant-coefficient non-relativistic polarized transport equation, with its analytical solution.

Our settings are consistent with these references [J. Dexter, 2016 MNRAS et al.], where the initial conditions for both tests are set as $I = Q = U = V = 0$ and the integration interval is selected as $\lambda \in (0, 3)$.

Test	j_I	j_Q	j_U	j_V	a_I	a_Q	a_U	a_V	r_Q	r_U	r_V
Emission/Absorption	2	1	0	0	1	1.2	0	0	0	0	0
Rotation	0	0.1	0.1	0.1	0	0	0	0	10	0	-4

表 1: The selection of parameters in the validation of analytical results.

To simplify the representation of the analytical solution, we analyze the effects of emission, absorption, and Faraday rotation separately.

Validation of analytical results

In **Coport**, we employ the 4th-order Runge-Kutta (RK4) method to tackle this issue, setting the absolute error tolerance at $\bar{\epsilon} = 1 \times 10^{-12}$. Fig. 3 illustrates the numerical outcomes alongside the analytical solutions for two distinct assessments, as well as the absolute discrepancies between the numerical and analytical results.

From the comparison between the numerical results and the analytical outcomes, it is evident that the numerical results provided by **Coport** are reliable. The examination of the absolute error reveals that the solver's results align well with our designated error tolerance.

Validation of analytical results

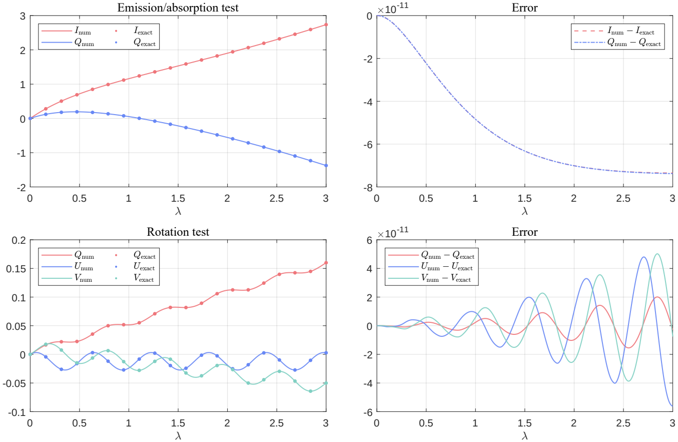

图 3: The first row corresponds to the outcomes derived from the emission/absorption examination, while the second row delineates the findings from the rotation test. The left column illustrates the evolution of Stokes parameters. The right column depicts the absolute discrepancy.

Validation of thin disc

We will conduct calculations using two distinct methods: one employing our **Coport** program and the other utilizing the Penrose-Walker (PW) constant for computation.

We adopt the evaluation metric utilized in the article [**Event Horizon Telescope** Collaboration 2023 APJ], specifically employing the normalized mean squared error (NMSE) to assess outcomes. The NMSE allows us to gauge the similarity between two images:

$$\text{NMSE}(A, B) = \frac{\sum_{i,j} |A(i,j) - B(i,j)|^2}{\sum_{i,j} |A(i,j)|^2} \,. \tag{23}$$

In this equation, $A(i,j)$ and $B(i,j)$ represent the values of a particular Stokes parameter at pixel (i,j) in the two images, respectively.

We divide the images generated by both methods into 16 subregions, each consisting of 512×512 pixels. Subsequently, we calculate the NMSE for each subregion individually.

Validation of thin disc

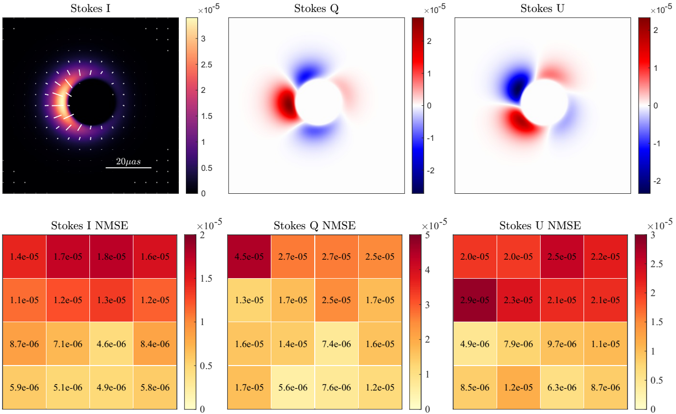

图 4: The results of the thin disk test are presented in two rows. The first row shows images of Stokes I, Q, and U generated using **Coport**. The second row features a plot of the NMSE, calculated by comparing the results from **Coport** with PW-constant computations across different regions.

Validation of the Thick Disk Model

- In the thick disk tests, we employ two distinct validation approaches. The first approach involves cross-validating results by using different numerical methods with varying convergence accuracies in **Coport**.
- The second approach, referred to as the **RAPTOR-like** code, involves the independent calculations of parallel transport of polarized vectors and the interaction with the plasma, similar to the RAPTOR code.
- Here, we are not directly using the RAPTOR code. Instead, we have independently developed a program for validation based on the theoretical framework of the RAPTOR code as outlined in [T. Bronzwaer, Z. Younsi, J. Davelaar, and H. Falcke, 2020 AA].

Validation of the Thick Disk Model

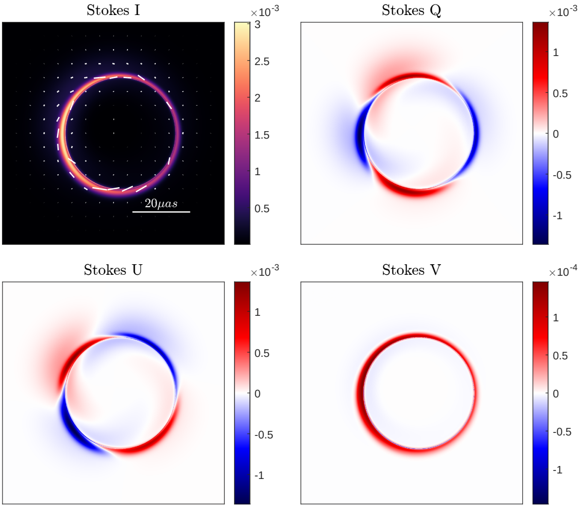

图 5: The resulting Stokes parameters I, Q, U, V are generated by the **Coport** . The pixel density is 1024×1024.

Validation of the Thick Disk Model

Stokes I NMSE

	RK4	Vern9	VCAB4
Midpoint	3.4e-04	2.7e-04	1.9e-04
RK4		4.8e-06	2.7e-05
Vern9			9.3e-06

Stokes Q NMSE

	RK4	Vern9	VCAB4
Midpoint	7.6e-03	7.8e-03	7.1e-03
RK4		1.5e-04	9.8e-05
Vern9			1.9e-04

Stokes U NMSE

	RK4	Vern9	VCAB4
Midpoint	8.8e-03	9.2e-03	9.4e-03
RK4		1.4e-03	2.3e-03
Vern9			1.4e-03

Stokes V NMSE

	RK4	Vern9	VCAB4
Midpoint	6.7e-04	6.8e-04	1.1e-03
RK4		5.7e-05	6.6e-04
Vern9			3.7e-04

图 6: Comparison of the normalized mean squared error (NMSE) of the results generated using different numerical methods in **Coport**.To facilitate a more intuitive understanding, we will apply shading to the cells in the table.

Validation of the Thick Disk Model

In this analysis, we maintain a fixed step size of $\Delta\lambda = 0.02$ for the RAPTOR-like code. We also compute the NMSE results between **Coport** and RAPTOR-like, as presented in Table 2.

NMSE I	NMSE Q	NMSE U	NMSE V
3.4×10^{-4}	1.4×10^{-2}	5.7×10^{-3}	1.2×10^{-2}

表 2: **Coport** vs. RAPTOR-like.

From the table, it can be observed that the highest order of NMSE is on the scale of only 10^{-2}, indicating consistency with the NMSE magnitudes reported in the GRMHD snapshot test outputs as described in [**Event Horizon Telescope Collaboration 2023 APJ**].

GRMHD Snapshot

Coport has developed an interface to visualize the numerical results obtained from GRMHD simulations.

We utilize HARM [C. F. Gammie, J. C. McKinney, and G. Toth 2003, APJ], an open-source GRMHD tool, to simulate the accretion process near a supermassive black hole.

Subsequently, **Coport** generates the corresponding polarization images.

Additionally, we use our self-developed RAPTOR-like code to image the data obtained from the same HARM simulations, thereby cross-validating the accuracy of our approach.

GRMHD Snapshot

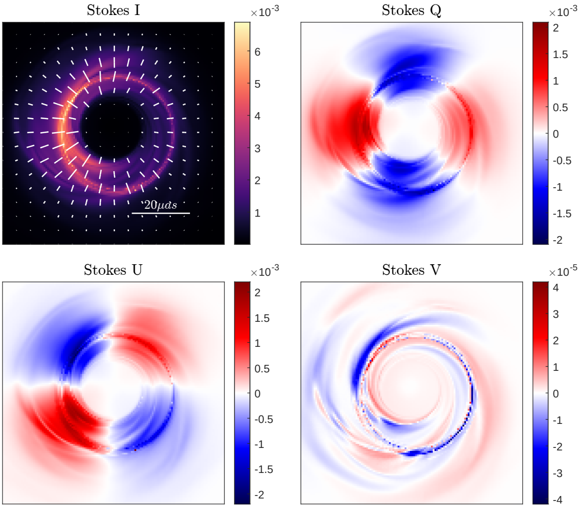

图 7: The resulting Stokes parameters I, Q, U, V of the GRMHD snapshot are generated by the **Coport** . The pixel density is 128 $\times$ 128.

GRMHD Snapshot

NMSE I	NMSE Q	NMSE U	NMSE V
3.8×10^{-3}	2.4×10^{-2}	1.8×10^{-2}	4.9×10^{-2}

表 3: **Coport** vs. RAPTOR-like.

The outcomes generated by **Coport** are presented in Fig. 7. Additionally, the disparities between the results produced by the **Coport** algorithm and the RAPTOR-like code are outlined in Table 3. Table 3 shows that the NMSE values are on the order of 10^{-2}. This again indicates consistency with the NMSE magnitudes reported in the GRMHD snapshot test outputs, as described in **[Event Horizon Telescope Collaboration 2023 APJ].**

Summary

Summary

- To improve our understanding of polarized observations in the environments with strong gravitational fields, we have developed a highly efficient algorithm named **Coport** for polarized radiative transfer across various spacetime frameworks..

Summary

- To improve our understanding of polarized observations in the environments with strong gravitational fields, we have developed a highly efficient algorithm named **Coport** for polarized radiative transfer across various spacetime frameworks..
- Our code addresses both gravitational effects and plasma interactions concurrently by solving the covariant polarized radiative transfer equation directly. Our formalism not only adeptly encapsulates the covariance inherent in the gravitational theory but also ensures high efficiency in numerical computations.

Summary

- To improve our understanding of polarized observations in the environments with strong gravitational fields, we have developed a highly efficient algorithm named **Coport** for polarized radiative transfer across various spacetime frameworks..
- Our code addresses both gravitational effects and plasma interactions concurrently by solving the covariant polarized radiative transfer equation directly. Our formalism not only adeptly encapsulates the covariance inherent in the gravitational theory but also ensures high efficiency in numerical computations.
- We have validated the accuracy and the precision of our new algorithms through multiple methods: comparing them with analytical solutions and validating them using both thin-disk and thick-disk models.

Summary

Coport is a novel instrument designed to analyze the radiative properties of diverse plasma models in arbitrary spacetimes.

These simulations aim to align with current and future observations of polarized radiation from relativistic plasma around black holes, neutron stars, and potentially other intriguing celestial objects.

Thank you!